Auxin-transporting ABC transporters are defined by a conserved D/E-P motif regulated by a prolylisomerase

Pengchao Hao[1], Jian Xia[1], Jie Liu[1], Martin Di Donato[1], Konrad Pakula[2,3], Aurélien Bailly[4], Michal Jasinski[2,5], and Markus Geisler[1,*]

From the [1]Department of Biology, University of Fribourg, Fribourg, Switzerland, [2]Department of Plant Molecular Physiology, Institute of Bioorganic Chemistry, Polish Academy of Sciences, Poznan, Poland, [3]NanoBioMedical Centre, Adam Mickiewicz University, Poznan, Poland, [4]Institute for Plant and Microbial Biology, Zurich, Switzerland, [5]Department of Biochemistry and Biotechnology, Poznan University of Life Sciences, Poznan, Poland

The plant hormone auxin must be transported throughout plants in a cell-to-cell manner to affect its various physiological functions. ABCB transporters are critical for this polar auxin distribution, but the regulatory mechanisms controlling their function is not fully understood. The auxin transport activity of ABCB1 was suggested to be regulated by a physical interaction with FKBP42/Twisted Dwarf1 (TWD1), a peptidylprolyl *cis-trans* isomerase (PPIase), but all attempts to demonstrate such a PPIase activity by TWD1 have failed so far. By using a structure-based approach, we identified several surface-exposed proline residues in the nucleotide binding domain and linker of Arabidopsis ABCB1, mutations of which do not alter ABCB1 protein stability or location but do affect its transport activity. P1008 is part of a conserved signature D/E-P motif that seems to be specific for auxin-transporting ABCBs, which we now refer to as ATAs. Mutation of the acidic residue also abolishes auxin transport activity by ABCB1. All higher plant ABCBs for which auxin transport has been conclusively proven carry this conserved motif, underlining its predictive potential. Introduction of this D/E-P motif into malate importer, ABCB14, increases both its malate and its background auxin transport activity, suggesting that this motif has an impact on transport capacity. The D/E-P1008 motif is also important for ABCB1-TWD1 interactions and activation of ABCB1-mediated auxin transport by TWD1. In summary, our data imply a new function for TWD1 acting as a putative activator of ABCB-mediated auxin transport by *cis-trans* isomerization of peptidyl-prolyl bonds.

The polar distribution of the plant hormone, auxin, is a unique, plant-specific process and the primary cause for the establishment of local auxin maxima and minima that trigger a plethora of physiological and developmental programs (1–3). The generation, control, and flexibility of these gradients require the coordinated action of members of at least three major auxin transporter families: the PIN-FORMED (PIN), the AUXIN1-RESISTANT1 (AUX1)/LIKE AUX1 (AUX1/LAX), and the ABC transporters of the B family (ABCBs) (4–6). In Arabidopsis, so-called long PINs (PIN1, 2, 3, 4, and 7) function as plasma membrane (PM) permeases (5), whereas cytoplasmic entry over the plasma membrane was shown to be dependent on AUX1/LAX proteins thought to function as high-affinity auxin-proton symporters (7, 8). In contrast, a subgroup of auxin-transporting ABCBs (referred to as ATAs in the following) functions as primary active (ATP-dependent) auxin pumps that are able to transport against steep auxin gradients (9–11).

Of the 22 full-size ABCB isoforms in Arabidopsis, ABCB1, 4, 6, 14, 15, 19, 20, and 21, were associated with polar auxin transport (12–17), however, only for ABCB1, 4, 6, 19, 20, and 21, transport activities were confirmed (11–13, 15, 16, 18–20). Interestingly, although Arabidopsis ABCB1, 6, 19, and 20 and tomato ABCB4 (21) were shown to function as specific auxin exporters, Arabidopsis ABCB4 and 21 (11, 13, 16, 19) and rice (*Oryza sativa)* ABCB14 (22) were suggested to function as facultative IAA importers/exporters. In contrast, Arabidopsis ABCB14 is considered a malate importer (23). Currently, it is not known how many of the remaining 15 full-size ABCBs and 7 half-size ABCBs in Arabidopsis function as well as auxin transporters (Fig. S1).

All characterized auxin transporters have been shown to be regulated on the transcriptional and nontranscriptional level (9, 24, 25). PM PINs and ABCBs were shown to be regulated by a partially overlapping subset of members of the AGC kinase family (26, 27). Whereas protein phosphorylation of the central PIN loop seems to alter both their polarity and transport activity (28), phosphorylation of the so-called ABCB linker has been described to result only in activity changes (26–28).

Further, PINs and ABCBs seem to be also regulated by protein-protein interaction with *cis-trans* peptidylprolyl isomerases (PPIases), which are formed by three evolutionary unrelated families: the cyclophilins, the FK506-binding proteins (FKBPs), and the parvulins (9). The cyclophilin, diageotropica (DGT/CypA), seems to decrease the functionality of PINs and their presence on the PM (29), although underlying mechanisms are far from being understood. Further, the parvulin PIN1At was shown to affect PIN1 polarity by means of its PPIase activity (30). In contrast, biogenesis of the ATAs, ABCB1, 4, 19, was found to depend on the FKBP42, twisted dwarf1 ((TWD1)/ultracurvata 2). The latter concept is based on the finding that ABCB1, 4, and 19 are retained on the ER and degraded in *twd1* (31, 32) (Fig. S9). This model is further supported by that fact that *twd1* and *abcb1,19* plants reveal widely overlapping but not entirely identical auxin-

This article contains supporting information.

* For correspondence: Markus Geisler, markus.geisler@unifr.ch.

Present address for Pengchao Hao: School of Agriculture and Biology, Shanghai Jiaotong University, Shanghai, China

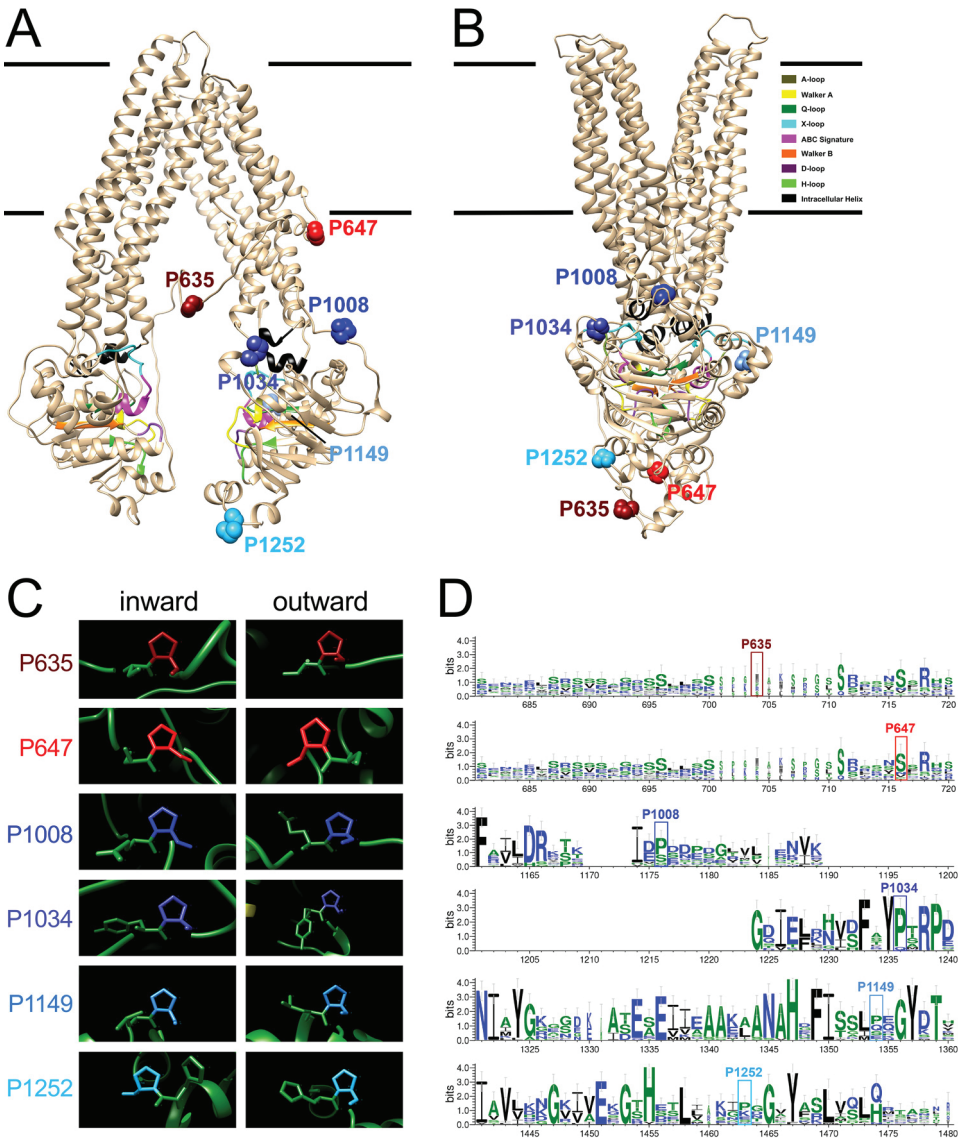

Figure 1. Mapping and conservation of surface-exposed proline residues on Arabidopsis ABCB1. *A* and *B*, surface-exposed prolines of the C-terminal nucleotide-binding fold (NBD2) and the linker are indicated as *blue* and *red* calottes, respectively, in the inward-open (*A*) and outward-open (*B*) conformations of Arabidopsis ABCB1 modeled on human PGP/ABCB1 as described elsewhere (47). Color code of functional NBD sequences can be deduced from the legend. *C*, close-up analyses of linker and NBD2 prolines indicate that all peptidyl-prolyl bonds are in *trans*. *D*, logo representation (WebLogo 3) of linker and NBD2 proline conservation in Arabidopsis after multiple sequence alignment with MUSCLE.

related phenotypes, including dwarfism and a nonhanded helical rotation of the epidermal cell files, designated as epidermal "twisting" (31, 32).

TWD1 was shown to interact physically via its PPIase/FK506-binding (FKB) domain with the C-terminal nucleotide-binding fold (NBD2) (Fig. 1) of ABCB1; however, the exact mechanism through which TWD1 regulates ABCB biogenesis and/or auxin transport is not yet known. High-molecular-weight FKBPs usually possess PPIase activity that is associated with the FKB domain (33, 34) and a chaperon activity that is thought to be linked with the tetratricopeptide repeat domain (33, 34). The latter was demonstrated for TWD1 (35); however, all attempts to demonstrate a PPIase activity on recombinant TWD1 protein have failed so far (36).

Interestingly, the proposed chaperone-like function for TWD1 during ER to plasma membrane trafficking of ABCBs is an analogy with the functional ortholog of TWD1/FBP42 in humans, FKBP38/FKBP8, that shares with TWD1/FKBP42 a unique mode of membrane anchoring (37, 38). FKBP38 promotes ER to plasma membrane delivery of the cystic fibrosis transmembrane conductance regulator, CFTR/ABCC7 (38). CFTR, belonging to ABCC/MRP family of ABC transporters, is a chloride channel whose malfunction is responsible for the genetic disorder mucoviscidosis (37). About 90% of all cystic fibrosis cases are associated with a specific single residue deletion, $CFTR^{\Delta Phe\text{-}508}$ (38, 39). This mutation results in a folding defect and the protein cannot traffic past the ER and is degraded via the proteasomal degradation pathway (40). It has been suggested that FKBP38 may play a dual role during these events by negatively regulating CFTR synthesis and positively regulating ER-associated maturation of WT and mutated form of CFTR (41). The latter functionality is PPIase-dependent (42)

and FKBP38 was shown to own a hidden, calmodulin-stimulated PPIase activity (37, 43, 44).

Functional FKBP-ABC interaction seems not to be limited to ABCCs as judged from the fact that the activity of murine ABCB4/MDR3 transporter expressed in *Saccharomyces cerevisiae* requires the presence of yeast FKBP12 (45). Interestingly, yeast FKBP12 seems to compete with TWD1 for regulation of Arabidopsis ABCB1 activity in yeast (26, 46), suggesting that this mode of action might be evolutionary, conserved over kingdoms. This is further supported by the finding that FKBP12 partially complements the *twd1* mutant phenotype (26).

Here, in an attempt to explore the relevance of putative proline residues that might be a substrate of a yet to be demonstrated PPIase activity of TWD1, we mapped putative surface prolines on the NBD2 of ABCB1 and tested their impact on ABCB1-mediated auxin transport activities. An essential D/E-P motif was identified that seems to be conserved in all so far described ABCBs that transport auxin and thus seems to define ATAs. The D/E-P1008 motif is important for ABCB1-TWD1 interaction and for TWD1-mediated activation of ABCB1 transport activity supporting a previously suggested scenario in that TWD1 acts as a positive modulator of ABCB1 transport activity by means of its putative PPIase activity.

Results

Identification of a conserved D/E-P motif in the C-terminal nucleotide-binding fold of ABCBs

Despite the fact that all attempts to demonstrate a PPIase activity on TWD1 were unsuccessful (36), we aimed in this study to test the impact of relevant proline residues on ABCB1 transport activity by using site-directed mutagenesis. To narrow down the number of candidate prolines, we focused on prolines that were potentially sterically accessible by TWD1 based on experimentally verified TWD1-ABCB1 contact sites. Yeast two-hybrid (36) and bioluminescence resonance energy transfer (BRET) (31, 46) analyses were allowed to limit the interacting site on ABCB1 to amino acid residues 980 to 1286 of the C-terminal nucleotide binding domain. Further, by using a valid structural model for Arabidopsis ABCB1 that was built on mouse ABCB1/PGP as a template (47), we were able to cut down the numbers of putative surface-exposed prolines to the four prolines Pro-1008, Pro-1034, Pro-1149, and Pro-1252 (Fig. 1). For doing so, we used the inward open conformation of ABCB1 (Fig. 1*A*) because we assumed that any activation of ABCB1 transport by TWD1 (26) should be occurring in this state. Finally, we included in our mutagenesis approach the two linker prolines, Pro-635 and Pro-647 (Fig. 1*A*), because ABCB linkers are thought to be very flexible and thus most likely are also accessible by TWD1 (26, 48). Another rationale was that Ser-634 was recently shown to be phosphorylated by the AGC kinase PINOID in an action that depended on TWD1, resulting in altered ABCB1 transport activity (26). Interestingly, despite the tremendous rearrangements known to occur between inward- and outward-facing ABCB conformations, all prolines (except Pro-647) remained surface-exposed also in the outward-facing conformation (Fig. 1*B*).

Web-based tools, such as CISPEPpred (http://sunflower.kuicr.kyoto-u.ac.jp/~sjn/cispep), predicted that all selected prolines except Pro-1034 would be in *trans* (not shown). A thorough manual investigation of the selected six proline residues using both inward-open and outward-open modeled conformers of ABCB1 revealed that all Cα-C-N-Cα bonds were actually in the *trans* conformations independent of the ABCB1 conformation (Fig. 1*C*). Sequence alignments with all 29 Arabidopsis ABCB isoforms indicated that the six prolines showed a variable degree of conservation. Whereas the linker prolines and the very C-terminal Pro-1252 showed a very low degree of conservation, the remaining three prolines that are part of the NBD2 were clearly more conserved (Fig. 1*D* and Fig. S2). A comparison between the proline-containing stretches of NBD2 and those of NBD1, known to evolve from each other by gene duplication (49), indicated that Pro-1008 but not the other three prolines seemed to be specific for NBD2 (Fig. S3).

Interestingly, we found that the presence of a D/E-P motif in the NBD2 correlated perfectly with auxin transport capacities of investigated Arabidopsis ABCBs diagnosed so far (Fig. S1). Intriguingly, sorghum DWARF3/ABCB1 (50), maize BRACHYTIC2/ABCB1 (50), rice ABCB14 (22), and tomato ABCB4 (21), all recently demonstrated to function as auxin transporters, also contain such a conserved D/E-P motif. In summary, it appears that auxin-transporting ABCBs contain a surface-exposed, conserved D/E-P motif in the NBD2.

Mutagenesis of the D/E-P1008 motif destroys the auxin-transport activity of ABCB1 without interfering with its ATPase activity or plasma membrane presence

Introducing single-point mutations in the NBDs of ABC transporters can have strong effects on protein stability, most likely because nonfunctional ABC transporters are recognized as such and degraded (51). To exclude an unwanted impact of these six proline mutations on ABCB1 secretion and/or protein stability, we semi-quantitatively analyzed their expression by agrobacterium-mediated leaf transfection of the tobacco, *Nicotiana benthamiana.* Confocal analyses of epidermal layers of leaves (Fig. 2*A*) and protoplasts prepared from those (Fig. S4) counterstained with the PM styryl dye, FM4-64, revealed that neutralization of the six prolines by glycine, allowing the peptide backbone to rotate, did not significantly alter ABCB1-YFP expression and location. These imaging data were confirmed by quantification of Western blots on microsomal fractions from three independent leaf infiltrations (Fig. 2*B*) revealing similar expression levels based on ratios of ABCB1-YFP and the PM marker, PIP2;1 (26).

Next, we quantified IAA export of mutated version of ABCB1 from protoplasts prepared from leaf-transfected tobacco (Fig. S4). Interestingly, except the Pro-1034 mutation all proline mutations revealed reduced IAA export to vector control level (Fig. 2*C*). This inhibitory effect was specific for IAA because transport of the diffusion control, benzoic acid (BA), was not affected by ABCB1 mutation (Fig. 2*D*). To test if proline mutations of the NBD2 and eventually also the linker had an effect on ATP hydrolysis by ABCB1, we quantified ATPase activity of microsomal fractions prepared from

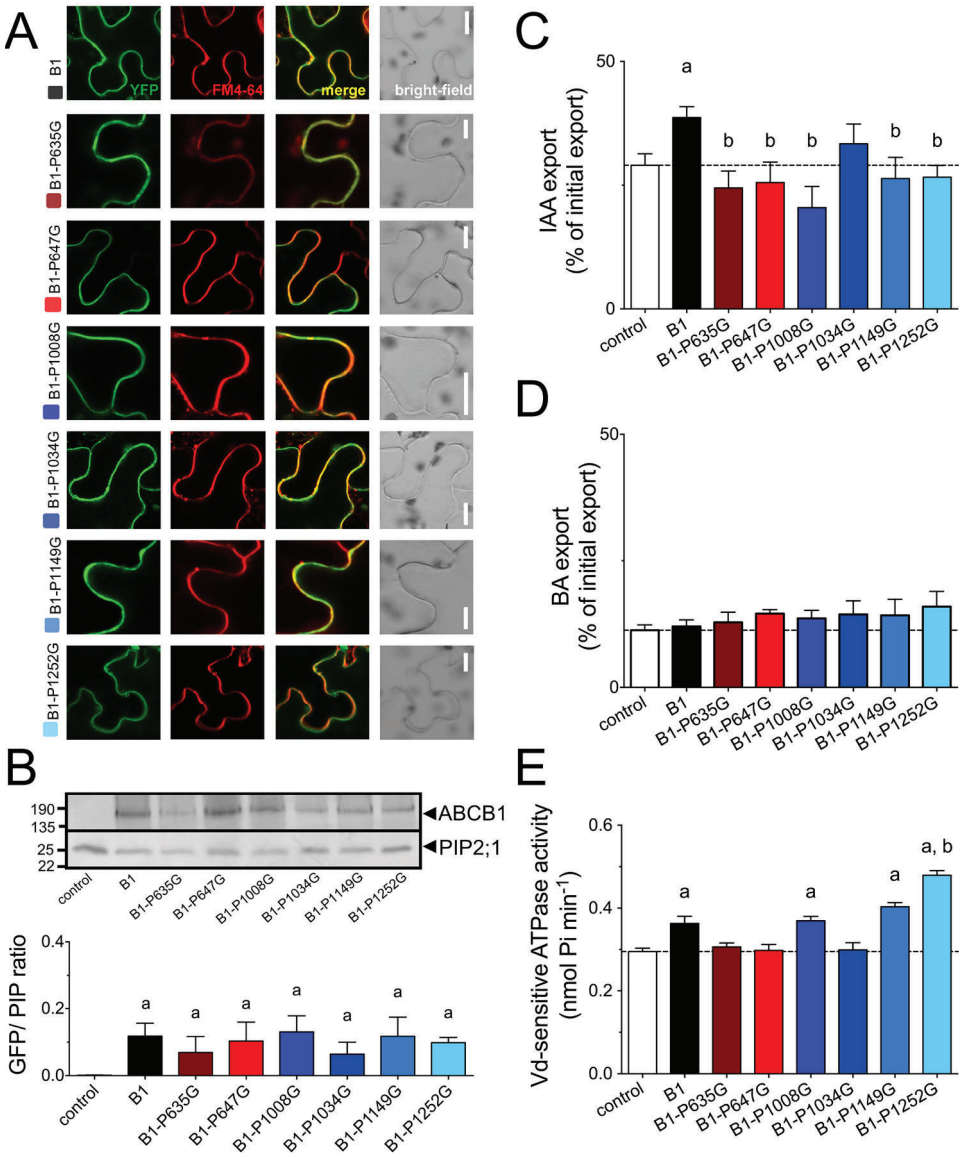

Figure 2. Mutation of most surface-exposed prolines in ABCB1 reduces IAA export. *A*, mutation of six surface-exposed prolines does not significantly alter expression and PM as revealed by confocal imaging of ABCB1-GFP of tobacco leaves transfected with ABCB1-GFP and stained with PM marker, FM4-64. *Bars*, 10 μM. *B*, proline mutation of ABCB1 does not significantly alter expression levels revealed by Western analyses of total microsomes prepared from tobacco leaves transfected with ABCB1 (*upper panel*). Microsomes were stained for GFP and plasma membrane marker, PIP2;1. ABCB1 expression was evaluated by calculating GFP/PIP ratios from three independent tobacco transfections (*lower panel*). *C* and *D*, IAA (*C*) and BA (*D*) export of protoplasts prepared from tobacco leaves transfected with WT and indicated proline mutants of ABCB1. *E*, vanadate (*Vd*)-sensitive ATPase activity of microsomal fractions prepared from tobacco leaves transfected with WT and indicated proline mutants of ABCB1; controls are in Fig. S6. Significant differences (unpaired *t test* with Welch's correction, $p < 0.05$) to vector control or ABCB1 are indicated by an "a" or a "b," respectively. Mean ± S.E.; $n \geq 4$ transport experiments generated from independent tobacco transfections.

transfected tobacco. ABCB1 expression significantly increased the fraction of vanadate-sensitive ATPase activity (Fig. 2*E*), which can be attributed to ABC transporters, whereas no significant difference between vector control and ABCB1 was found for the vanadate-insensitive fraction or in the absence of ATP (Fig. S5). ABCB1-mediated ATPase activity was not stimulated by the native substrate, IAA, as found for many ABC transporters (52). Interestingly, loss of IAA transport for both linker mutations correlated with a loss of ATPase activity, supporting the proposed impact of the regulatory linker on the NBD motions (53). The very C-terminal proline mutation showed increased ATPase activity, which indicates that this mutation might have resulted in an uncoupling of transport from ATPase activity. The most interesting finding, however, was that P1008G mutation did abolish IAA transport without affecting ABCB1 ATPase activity, indicating that Pro-1008 most likely interferes with ABCB1 activity regulation by a mode that is essentially independent of ATP hydrolysis.

In light of the proposed, essential function of the D/E-P1008 motif for auxin transport, we asked if the D/E prior to the proline was likewise critical. Interestingly, alanine substitution of Glu-1007 also reduced IAA transport but not BA transport activity (Fig. 3, *A* and *B*) without changing significantly ABCB1 expression or location (Fig. 3*D*). Similarly, E1007A mutation had no impact on ABCB1 ATPase activity (Fig. 3*C*), indicating in summary that both residues of the D/E-P1008 motif

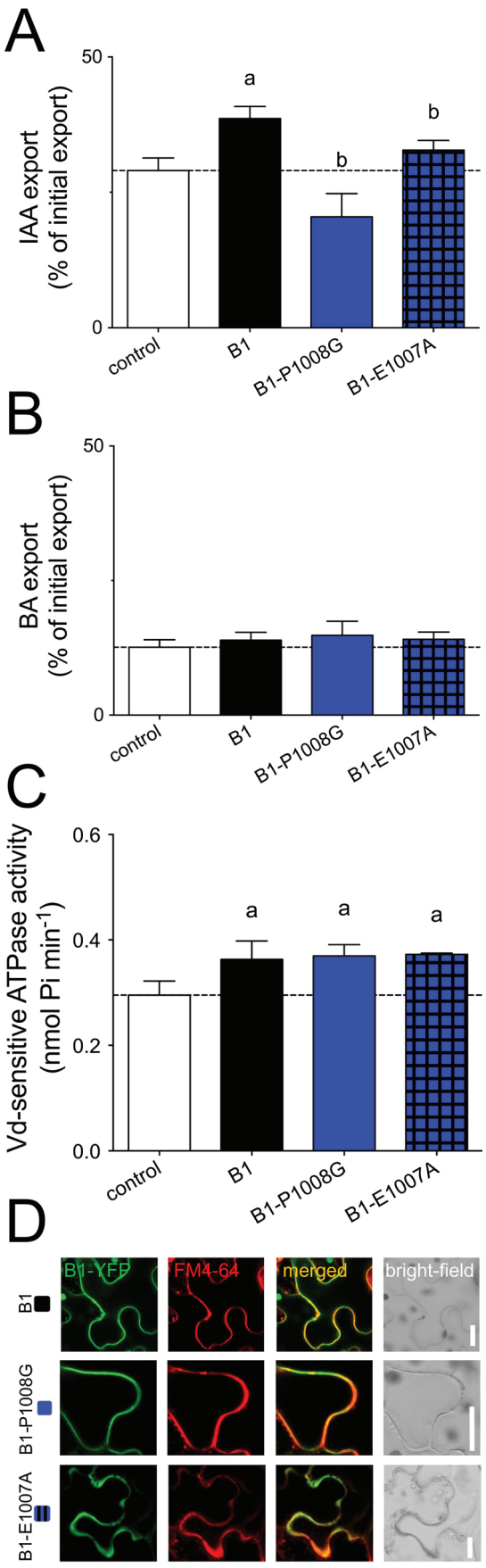

Figure 3. Mutagenesis of the D/E-P1008 motif abolishes the auxin-transport activity of ABCB1 without interfering with its ATPase activity or PM location. *A* and *B*, IAA (*A*) and BA (*B*) export of protoplasts prepared from tobacco leaves transfected with WT and indicated E-P1008 mutations of ABCB1. *C*, ATPase activity of microsomal fractions prepared from tobacco leaves transfected with WT and indicated E-P1008 mutations of ABCB1. Significant differences (unpaired *t test* with Welch's correction, $p < 0.05$) to vector control or ABCB1 are indicated by an "a" or a "b," respectively. Mean ± S. E.; $n \geq 4$ transport experiments generated from independent tobacco transfections. *D*, E-P1008 mutants of ABCB1 are expressed at similar level on the plasma membrane revealed by confocal imaging of ABCB1-GFP of tobacco leaves transfected with ABCB1-GFP and stained with PM marker, FM4-64. *Bars*, 10 μM. Note that B1 and B1-P1008G panels have been reused from Fig. 2*A*.

are essential for ABCB1 IAA transport in a mode that most likely does not involve the ATPase activity of NBD2.

Introduction of a D/E-P motif into malate importer ABCB14 increases its background auxin transport activity

The only Arabidopsis ABCB that does not transport auxin but for that a transport activity has been proven is ABCB14 functioning as a PM malate importer (23). ABCB14 contains P-P991 instead of the D/E-P. PM expression of WT ABCB14 in tobacco resulted in slightly reduced malate export (an indicative for enhanced import) verifying previous studies (23) but also a slightly increased IAA export, although both differences were not significantly different from vector control (Fig. 4, *A* and *B*). Interestingly, correction of the P-P991 into E-P991 both significantly enhanced malate import by ABCB14, as well as IAA export activity without changing its PM location (Fig. 4*C*). In summary, these datasets indicate that introduction of a D/E-P motif into a nonauxin transporting ABCB increases its native (malate) transport capacity and thus most likely also a background IAA export activity that was suggested recently (17).

The D/E-P1008 motif is important for ABCB1 interaction with TWD1

The findings above left us with the possibility that the D/E-P1008 motif in ABCB1 was not only essential for ABCB1 activity regulation but eventually also for interaction with TWD1, described as a regulator of ABCB1 transport activity by protein-protein interaction (26, 31, 46, 54). In fact, it was shown that dissociation of TWD1 from ABCB1 by the auxin efflux inhibitor 1-*N*-naphthylphthalamic acid disrupted the regulatory impact of TWD1 on ABCB activity (46). To test the impact of the E-P1008 motif on TWD1-ABCB1 interaction, we measured TWD1-ABCB1 interaction by employing an established microsome-based BRET assay (31, 46). In short, TWD1 was C-terminal tagged with bioluminescent *Renilla* luciferase (Rluc) as donor and co-transfected with ABCB1-YFP as acceptor in tobacco. This pair of donor and acceptor has an approximate Förster distance of 4.4 nm, which is generally considered a direct physical interaction (55). Therefore, BRET, in contrast to co-IPs, does, besides the advantage of being quantitative, also allow for a differentiation between direct or indirect interactions. As shown before, co-expression of ABCB1-YFP and TWD1-Rluc resulted in significant BRET ratios, whereas the negative controls, AUX1-YFP or YFP alone, did not (Fig. 5*A*). Interestingly, co-expression of ABCB4-YFP with TWD1-Rluc also resulted in comparable BRET ratios (Fig. 5*A*) without significantly altering expression or location of both partners (Fig. S6). This supports the

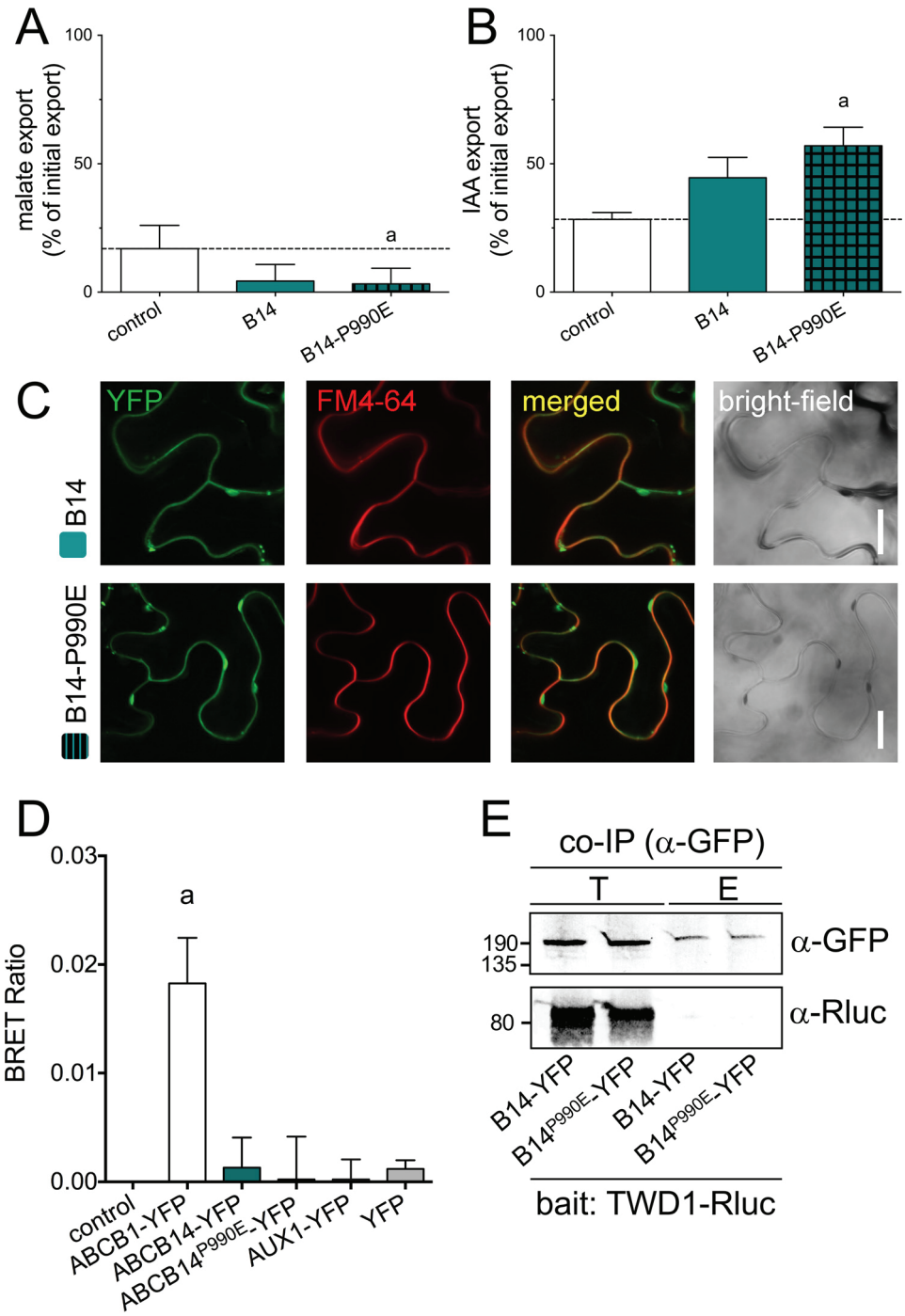

Figure 4. Introduction of an E-P motif into malate importer, ABCB14, increases its transport activity. *A* and *B*, simultaneous malate (*A*) and IAA (*B*) export of protoplasts prepared from tobacco leaves transfected with WT and P990E-mutated ABCB14 (B14). Significant differences (unpaired *t test* with Welch's correction, $p < 0.05$) to vector control are indicated by an "a." Mean ± S.E.; $n \geq 4$ transport experiments generated from independent tobacco transfections. *C*, P990E mutation does not alter significantly expression or plasma membrane location of ABCB14 revealed by confocal imaging of ABCB1-GFP of tobacco leaves transfected with ABCB1-GFP and stained with PM marker, FM4-64. *Bars*, 10 μM. *D*, BRET analyses of microsomal fractions prepared from tobacco leaves co-transfected with TWD1-Rluc and WT and P990E mutation of ABCB14-GFP. AUX1-YFP/TWD1-Rluc and YFP/TWD1-Rluc were used as negative and ABCB1YFP/TWD1-Rluc as positive controls. Significant differences (unpaired *t test* with Welch's correction, $p < 0.05$) to control (TWD1-Rluc alone) are indicated by an "a." Mean ± S.E.; $n = 3$ BRET measurements from 3 independent tobacco transfections. *E*, co-immunoprecipitation of TWD1-Rluc using WT and P990E mutation of ABCB14-YFP as a bait. Co-IP was performed from microsomal fractions prepared from tobacco leaves co-transfected with indicated combinations. Total input (*T*) and elution (*E*) were probed against anti-GFP and anti-Rluc detecting ABCB14-YFP and TWD1-Rluc, respectively.

concept that lack of ABCB4-TWD1 interaction is the cause of ABCB4 de-regulation in *twd1* (31, 32).

Excitingly, both mutation of P1008G (~17% reduction) and E1007A in ABCB1-YFP (~39% reduction) decreased interaction with TWD1-Rluc, although only the latter was significant (Fig. 5*A*). Co-expression of TWD1 with mutant version of ABCB1 did not significantly alter expression or PM location of both partners excluding unwanted secondary effects

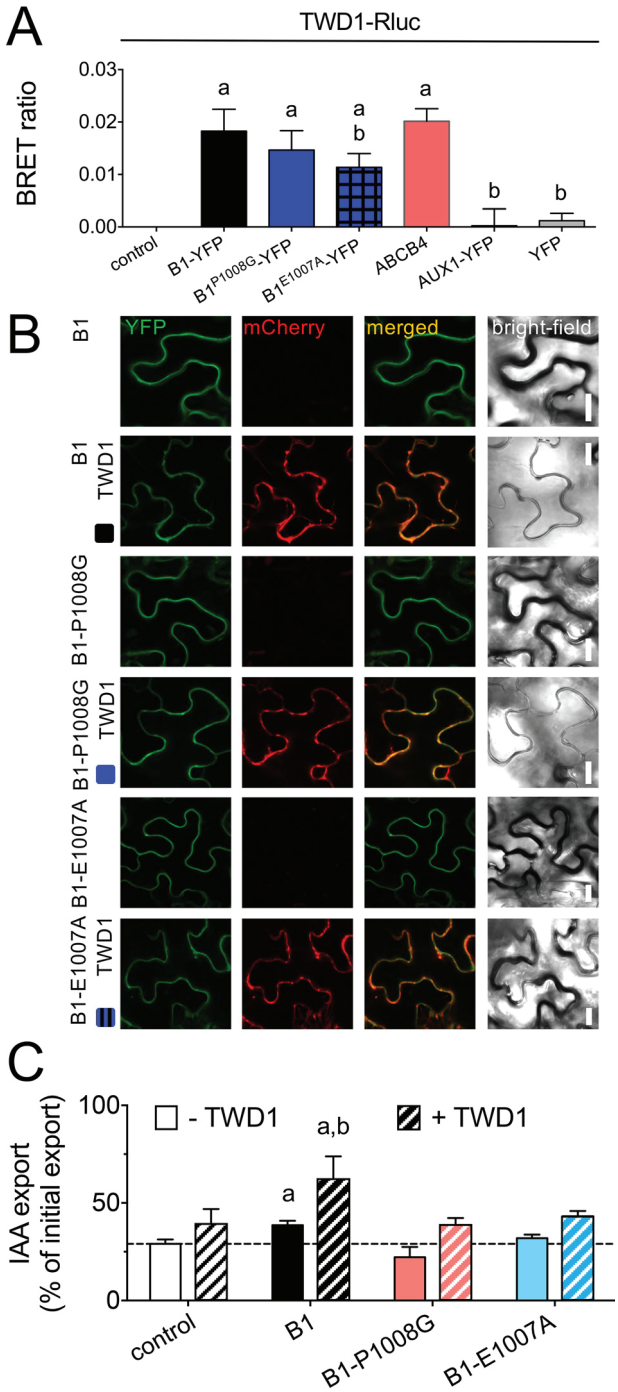

Figure 5. The D/E-P1008 motif in ABCB1 is important for interaction with TWD1 and regulation by TWD1. *A*, BRET analyses of microsomal fractions prepared from tobacco leaves co-transfected with TWD1-Rluc and WT and indicated E-P1008 mutations of ABCB1-YFP. AUX1-YFP/TWD1-Rluc and YFP/TWD1-Rluc were used as negative controls. Significant differences (unpaired *t test* with Welch's correction, $p < 0.05$) to control (TWD1-Rluc alone) are indicated by an "a," significant differences to ABCB1-YFP/TWD1-Rluc by a "b." Mean ± S.E.; $n = 3$ BRET measurements from 3 independent tobacco transfections. *B*, both E1007A and P1008G mutant versions of ABCB1-YFP co-localize with TWD1-mCherry on the epidermal PM of tobacco leaves after co-transfection. *Bars*, 10 μM. *C*, IAA export of protoplasts prepared from tobacco leaves co-transfected with TWD1-mCherry and WT or indicated D/E-P1.008 mutations of ABCB1-YFP. Significant differences (unpaired *t test* with Welch's correction, $p < 0.05$) to vector control or ABCB1-YFP are indicated by an "a" or a "b," respectively. Mean ± S.E.; $n = 4$ transport measurements from 4 independent tobacco transfections.

(Fig. 5*B*). In summary, these data indicate that the E-P1008 motif is important but not essential for ABCB1-TWD1 interaction.

The E-P1008 motif in ABCB1 is essential for ABCB1 activation by TWD1 and auxin transport activity in planta

To show that the described activation of ABCB1-mediated IAA export caused by TWD1 interaction depends on the E-P1008 motif, we quantified IAA export from protoplasts prepared from tobacco leaves co-infiltrated with TWD1-mCherry and WT and mutant versions of ABCB1-YFP. As described before (26), TWD1-mCherry enhanced slightly IAA export of vector controls, most likely because of activation of tobacco-endogenous ABCBs (Fig. 5*C*). In contrast, co-transfection of TWD1-mCherry with WT ABCB1-YFP significantly enhanced IAA export. Strikingly, the activating effect of TWD1-mCherry was absent with Glu-1007 and Pro-1008 mutations of ABCB1-YFP, clearly indicating that the E-P1008 motif in ABCB1 is essential for the regulatory impact provided by TWD1.

Finally, to test the importance of the E-P1008 motif *in planta*, we expressed WT and E1007A and P1008G mutant versions of ABCB1 in *abcb1-1* and Col WT under its native promoter (ABCB1:ABCB1-GFP) and a constitutive one (35S:ABCB1-YFP), respectively. As expected, complementation of the *abcb1-1* mutant with WT but not both mutant versions rescued IAA efflux to Was WT levels (Fig. 6*A*). In agreement, constitutive overexpression in Col WT revealed enhanced IAA export compared with WT only for WT ABCB1 but not for both mutants (Fig. 6*B*). Like in tobacco, no differences were found with the diffusion control, benzoic acid (Fig. S7). Importantly, confocal analyses of mutant versions of ABCB1:ABCB1-GFP in *abcb1-1* (Fig. 6*C*) and 35S:ABCB1-YFP in Col WT (Fig. 6*D*), respectively, revealed no significant differences in ABCB1 expression and location compared with WT ABCB1. In summary, these datasets underline the notion that the D/E-P1008 motif in auxin-transporting ABCBs is essential for auxin transport activity *in planta.*

Discussion

A conserved D/E-P motif in the C-terminal nucleotide-binding domain defines ATAs

By using a structure-based approach we have identified a series of surface-embedded proline residues in the NBD2 and linker of Arabidopsis ABCB1 (Fig. 1) that do not alter ABCB1 protein stability or location but its catalytic transport activity (Figs. 2 and 3). Of special interest was Pro-1008 because we uncovered that this proline is part of a signature D/E-P motif that seems to be specific for ATAs. Besides the proline, also mutation of the acidic moiety prior to the proline abolishes auxin transport activity by ABCB1 in the heterologous tobacco system (Fig. 3) as well as *in planta* (Fig. 6). So far, all Arabidopsis ABCBs for that auxin transport were shown carry this conserved motif underlining its diagnostic potential. Interestingly, this motif does not seem to be restricted to dicots because it was also found in the monocot ATAs, sorghum DWARF3/ABCB1 (50), maize BRACHYTIC2/ABCB1 (50), and rice ABCB14 (22). The D/E-P signature was further found in all five

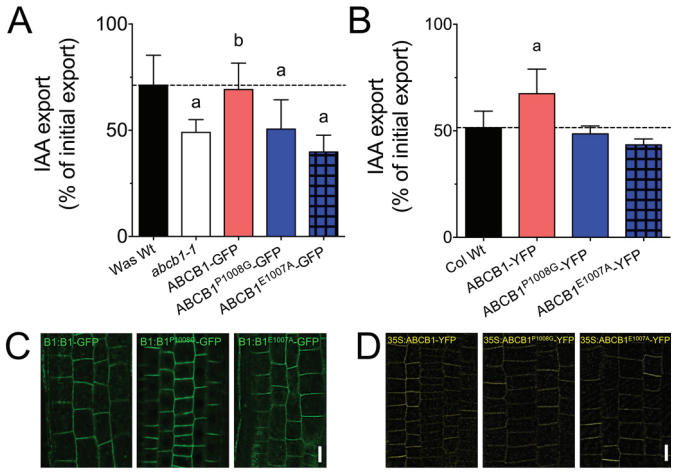

Figure 6. The D/E-P1008 motif in ABCB1 is essential for auxin transport activity *in planta*. *A*, IAA export of protoplasts prepared from *abcb1-1* transformed with WT or indicated E-P1008 mutations of ABCB1-GFP expressed under its native promoter (ABCB1:ABCB1-GFP). Significant differences (unpaired *t test* with Welch's correction, $p < 0.05$) to WT or *abcb1-1* are indicated by an "a" or a "b," respectively. Mean ± S.E.; $n = 4$ transport measurements from 4 independent protoplast preparations. Benzoic acid diffusion controls are in Fig. S7. B, IAA export of protoplasts prepared from Col WT transformed with WT or indicated E-P1008 mutations of ABCB1YFP expressed under a constitutive promoter (^{35}S:ABCB1-YFP). Significant differences (unpaired *t test* with Welch's correction, $p < 0.05$) to WT are indicated by an "a." Mean ± S.E.; $n = 4$ transport measurements from 4 independent protoplast preparations. Benzoic acid diffusion controls are in Fig. S7. *C* and *D*, confocal analyses of WT and mutant versions of ABCB1:ABCB1-GFP in *abcb1-1* (*C*) or ^{35}S:ABCB1-YFP in Col WT (*D*), respectively, revealed no significant differences in ABCB1 expression and location. *Bars*, 10 μM.

ABCBs of the Arabidopsis ABCB15-22 cluster (Fig. S1) for that no auxin transport data have yet been published. As a proof of concept, we verified specific IAA transport for all five ABCBs, indicating that most likely 11 of 22 full-size Arabidopsis ABCBs do transport auxin.[6]

To further validate our assumption, we corrected a P-P991 motif in Arabidopsis ABCB14 that was previously proposed (beside ABCB15) to promote auxin transport because inflorescence stems in both mutants showed a reduction in polar auxin transport (17). Mutation of P990E significantly increased a background auxin export activity on ABCB14 (Fig. 4), indicating that this mutation might have an impact on substrate specificity. This concept is indirectly supported by NBD mutations in the yeast ABCG-type transporter PDR5 that altered, besides transport capacity, also substrate specificity without changing the ATPase activity (56). A more likely option, however, is that mutation of this motif enhances the transport capacity in general, which is supported by the fact that the P990E mutation in ABCB14 also promotes malate import (Fig. 4).

A new mode of ABC transporter regulation by cis-trans isomerization of peptidyl-prolyl bonds via FKBPs?

In contrast to all other proline mutations, P1008G and E1007A mutations both did only affect auxin transport but not ATPase activity of ABCB1 (Figs. 2 and 3). A rationale for this finding is given by the fact that this motif, in contrast to most other prolines, is distant to the elements that are responsible for ATP binding and hydrolysis, like Walker A and B motifs (Fig. 1 and Fig. S8). Instead, E-P1008 lies in proximity and in between intracellular/coupling helices 2 and 3, establishing the connection between intracellular loops ICL2 and ICL3 and the NBD2 (Fig. 1 and Fig. S8) (57). Mutations in intracellular/coupling helices in human ABCB1 close to a well-conserved phenylalanine were reported to lead to dysfunctionality of the protein and its degradation (58). In Arabidopsis ABCB1, mutation of Phe-792, part of the coupling helix 3, leads to reduced binding of the noncompetitive auxin transport inhibitor BUM, thought to bind to this region of NBD2 (59). Further, many mutations of ABCC7/CFTR in the ICL2 and ICL4 are associated with cystic fibrosis (60).

However, an alternative but also plausible scenario is that mutation of P1008G and/or P1007E has a direct, steric impact on positioning of TMH12 that is connected via a short α-helix with this motif (Fig. S8). A recent analysis of the surface residues surrounding the putative IAA binding region 3 revealed a direct involvement of TMH12 in IAA binding in analogy to human ABCB1 (47). This proposes a scenario in that TMH12 might be slightly dislocated upon a transient E-P1008 isomerization opening the central substrate cavity. This scenario is supported by normal mode analysis of protein dynamics simulations using DynaMut (http://biosig.unimelb.edu.au/dynamut) revealing that P1008G (but not Glu-1007) mutation has a significant effect on ABCB1 local rigidity (not shown). In summary, this supports the idea that structural changes triggered by proline isomerization via TWD1 in a loop close to or in the ICLs connecting transmembrane domains with NBDs might have a momentous impact on ABCB transport activity that is absent in the E-P1008 mutants.

Another interesting finding was that the E-P1008 motif is not only indispensable for ABCB1 transport but also important, although not essential, for ABCB1 interaction with TWD1 (Fig. 5). Remarkably, besides the proline, also mutation of the acidic moiety prior to the proline leads to reduced binding of TWD1, which might indicate that both residues are an essential part of the TWD1 docking surface on the NBD2 of ABCB1. These two lines of evidence further support a previously suggested scenario in that TWD1 acts as a positive modulator of ABCB1 transport by means of its catalytic PPIase activity (9, 26, 36) (Fig. S9). This activity, although not experimentally verified for TWD1, is usually associated with its PPIase domain that was shown to physically interact with a stretch of the mapped ABCB1 C terminus (36). Strikingly, the functional human ortholog of FKBP42/TWD1, FKBP38, was demonstrated to have an impact on the biogenesis of human CFTR/ABCC7 (37). This action was shown to depend on a hidden PPIase activity on FKBP38 that was uncovered to require calmodulin activation (43). Whether TWD1 does also harbor such a calmodulin-stimulated PPIase activity is currently unknown but can now be tested, especially in knowledge of a putative *in vivo* peptide substrate.

Another open question is if all ATAs do physically interact with TWD1 or other, not yet identified, PPIases. We here show that TWD1, beside with ABCB1, 19 (12, 36, 46), also interacts with ABCB4 (Fig. 4), whose PM presence was shown to depend on TWD1 (31, 32). Interestingly, correction of a P-P991 into an

[6] P. Hao, J. Chen, S. Vanneste, E. Shani, M. Geisler, and T. Beeckman, unpublished data.

E-P991 motif in ABCB14 increased transport capacities but did not restore interaction with TWD1 shown by BRET and co-IP (Fig. 4, *D* and *E*), indicating that interaction is provided by a structurally conserved surface that extends these two amino acids.

However, in contrast to the described CFTR/FKBP38 model our data suggest a mode of ABC transporter regulation in that *cis-trans* isomerization catalyzed by the PPIase activity of TWD1 would lead to a transient activation of auxin transport activity (Fig. S9). This scenario is supported by our finding that IAA transport of WT ABCB1 but not of E1007A and P1008G mutant versions of ABCB1-YFP can be activated by TWD1 (Fig. 5*C*). The difference and novelty of this, so far not demonstrated, mode of transporter regulation would lie in the fact that deactivation would not require a second enzymatic step (like for dephosphorylation) but would happen by spontaneous re-isomerization known to occur slowly (in seconds to minutes) because of the high energy barrier imposed by the partial double bond character of the peptide bond (61). Interestingly, also for HsCFTR/ABCC7, a mutation of prolines was shown to alter its channel properties (62). Strikingly, Pro-1008 of AtABCB1 seems to be conserved and surface exposed also in CFTR (Pro-1175) (Fig. S8, *A–C*) but also in AtABCC1/2, both shown to interact with and to be regulated by TWD1 (63) (Fig. S8*C*). Moreover, in the human breast cancer resistance protein, BCRP/ABCG2, mutation of Pro-392, located at the transmembrane domain–NBD interface, altered transport activity and substrate specificity (64). Currently, it is unclear if these X-P bonds are also folded by FKBPs; if so these data would suggest that this mode of transporter regulation is more frequent than thought.

Experimental procedures

Auxin transport measurements

Simultaneous ^{3}H-IAA and ^{14}C-BA or ^{14}C-malic acid (malate) export from tobacco (*N. benthamiana*) mesophyll protoplasts was analyzed as described (26). Tobacco mesophyll protoplasts were prepared 4 days after agrobacterium-mediated transfection of WT and indicated mutated versions of 35*S:ABCB1-YFP* (26) or 35*S:ABCB14-GFP* (23). In some cases, 35*S:ABCB1-YFP* was co-expressed with 35*S:TWD1-mCherry*. Relative export from protoplasts is calculated from exported radioactivity into the supernatant as follows: (radioactivity in the protoplasts at time $t = x$ min.) − (radioactivity in the supernatant at time t = 0) * (100%)/(radioactivity in the supernatant at t = 0 min); presented are mean values from more than four independent transfections.

Arabidopisis thaliana ecotype Col WT or *abcb1-1/pgp1-1* (in Was WT) was transformed by floral dipping with WT and mutant versions of ^{35}*S:ABCB1-YFP* (26) or *ABCB1:ABCB1-GFP* (65), respectively. Homozygous lines were isolated by progeny analyses and used for simultaneous ^{3}H-IAA and ^{14}C-BA export from mesophyll protoplasts as described in Ref. 26.

Site-directed mutagenesis

Point mutations in *ABCB1* were introduced into ^{35}*S:ABCB1-YFP* (26) and ^{35}*S:ABCB14-GFP* (23) using the QuikChange Lightning Site-Directed Mutagenesis Kit (Agilent).

ABCB1-TWD1 interaction analyses

ABCB1 co-immunoprecipitation analyses using anti-GFP micro beads (Miltenyi Biotec, Germany) were carried using microsomal fractions prepared from Agrobacterium–co-infiltrated *N. benthamiana* in triplicates as described recently (66).

For BRET analysis, *N. benthamiana* leaves were Agrobacterium co-infiltrated with indicated BRET construct combinations (or corresponding empty vector controls) and microsomal fractions were prepared 4 days after inoculation. BRET signals were recorded from microsomes (each ~10 μg) in the presence of 5 μM coelenterazine (Biotium Corp.) using the Cytation 5 image reader (BioTek Instruments), and BRET ratios were calculated as described previously (31). The results are the average of 20 readings collected every 30 s, presented as average values from a minimum of three independent experiments (independent Agrobacterium infiltrations) each with four technical replicates.

Confocal laser scanning imaging

For confocal laser scanning microscopy work, an SP5 confocal laser microscope was used. Confocal settings were set to record the emission of GFP (excitation 488 nm, emission 500–550 nm), YFP (excitation 514 nm, emission 524–550 nm), mCherry (excitation 587 nm, emission 550–650nm), and FM4-64 (excitation 543 nm, emission 580–640 nm).

Structure, sequence, and phylogenetic analyses

The homology-modeled structure for Arabidopsis ABCB1 (GenBank: NP_181228) recently modeled on the high-resolution P-glycoprotein ABCB1 structure (PDB ID: 3G5U) from *Mus musculus* (MmABCB1) was utilized as a template throughout this study (47). Human CFTR/ABCC7 (GenBank: NP_000483.3) was modeled on zebrafish CFTR (PDB ID: 5TSI) using iTasser (https://zhanglab.ccmb.med.umich.edu/I-TASSER) because human CFTR did not contain structural information for the position relevant for D/E-P1.008. All structure figures were prepared and displayed using UCSF Chimera (https://www.cgl.ucsf.edu/chimera).

A phylogenetic analysis of Arabidopsis full-size ABCB transporter family members was performed by constructing maximum likelihood trees using PhyML 3.0 (http://www.atgc-montpellier.fr/phyml) based on the amino acid sequences aligned using MUSCLE (https://www.ebi.ac.uk/Tools/msa/muscle/). The graphic representation of the patterns within a multiple sequence alignment of selected α-helices were done with WebLogo 3 (http://weblogo.threeplusone.com).

Measurement of ATPase activity

Vanadate-sensitive ATPase activity of WT and mutant ABCB1 was measured from microsomes (0.06 μg/μl) prepared from transfected tobacco plants using the colorimetric

determination of orthophosphate released from ATP as described previously (67). Briefly, microsomes were added to ATPase buffer (20 mM MOPs, 8 mM $MgSO_4$, 50 mM KNO_3, 5 mM NaN_3, 0.25 mM Na_2MoO_4, 2.5 mM phosphoenolpyruvate, 0.1% pyruvate kinase) in the presence and absence of 0.5 mM sodium *ortho*-vanadate. The reaction was started by the addition of 15 mM ATP and incubated at 37°C for 15 min and 30 min with shaking. The stopping/ascorbate mixture was added to each well to terminate the reaction and after 10 min, the reaction mix was transferred into a stabilizing solution and incubated at room temperature for 1 h. The amount of P_i released was quantified with a colorimetric reaction, using a Cytation 5 reader (BioTek Instruments).

Data analysis

Transport data were statistically analyzed using Prism 7.0 (GraphPad Software, San Diego, CA). Unpaired *t test* with Welch's correction was used throughout this study, and mean values with a $p < 0.05$ were considered as significantly different.

Data availability

All data are contained within the manuscript.

Acknowledgments—We thank L. Charrier for excellent technical assistance and Y. Lee for the ^{35}S:ABCB14-GFP plasmid.

Author contributions—P. H., J. X., J. L., M. D. D., K. P., A. B., and M. G. data curation; P. H., J. X., J. L., M. D. D., K. P., A. B., and M. G. formal analysis; P. H., A. B., M. J., and M. G. writing-review and editing; A. B. and M. G. conceptualization; M. J. resources; M. J. and M. G. supervision; M. G. funding acquisition; M. G. validation; M. G. investigation; M. G. methodology; M. G. writing-original draft; M. G. project administration.

Funding and additional information—This work was supported by Swiss National Fund Grant 31003A-165877/1 and ESA CORA grant LIRAT (to M. G.). This work was also supported by the Polish National Center for Research and Development Ph.D. program POWR.03.02.00-00-1032/16 (to K. P.).

Conflict of interest—The authors declare that they have no conflicts of interest with the contents of this article.

Abbreviations—The abbreviations used are: ABCB, ATP-binding cassette protein subfamily B; PM, plasma membrane; IAA, indole-3-acetic acid; PPIase, *cis-trans* peptidyl-prolyl isomerase; ER, endoplasmic reticulum; NBD, nucleotide-binding domain; CFTR, cystic fibrosis transmembrane conductance regulator; BRET, bioluminescence resonance energy transfer; BA, benzoic acid; PGP, P-glycoprotein; ICL, intracellular loop; Rluc, *Renilla* luciferase; co-IP, co-immunoprecipitation.

References

1. Sorefan, K., Girin, T., Liljegren, S. J., Ljung, K., Robles, P., Galván-Ampudia, C. S., Offringa, R., Friml, J., Yanofsky, M. F., and Østergaard, L. (2009) A regulated auxin minimum is required for seed dispersal in Arabidopsis. *Nature* **459,** 583–586 CrossRef Medline
2. Robert, H. S., and Friml, J. (2009) Auxin and other signals on the move in plants. *Nat. Chem. Biol.* **5,** 325–332 CrossRef Medline
3. Pařízková, B., Pernisová, M., and Novák, O. (2017) What has been seen cannot be unseen—detecting auxin in vivo. *Int. J. Mol. Sci.* **18,** 2736 CrossRef Medline
4. Naramoto, S. (2017) Polar transport in plants mediated by membrane transporters: Focus on mechanisms of polar auxin transport. *Curr. Opin. Plant Biol.* **40,** 8–14 CrossRef Medline
5. Park, J., Lee, Y., Martinoia, E., and Geisler, M. (2017) Plant hormone transporters: What we know and what we would like to know. *BMC Biol.* **15,** 93 CrossRef Medline
6. Geisler, M. (2018) Seeing is better than believing: Visualization of membrane transport in plants. *Curr. Opin. Plant Biol.* **46,** 104–112 CrossRef Medline
7. Bennett, M. J., Marchant, A., Green, H. G., May, S. T., Ward, S. P., Millner, P. A., Walker, A. R., Schulz, B., and Feldmann, K. A. (1996) Arabidopsis AUX1 gene: A permease-like regulator of root gravitropism. *Science* **273,** 948–950 CrossRef Medline
8. Swarup, K., Benková, E., Swarup, R., Casimiro, I., Péret, B., Yang, Y., Parry, G., Nielsen, E., De Smet, I., Vanneste, S., Levesque, M. P., Carrier, D., James, N., Calvo, V., Ljung, K., *et al.* (2008) The auxin influx carrier LAX3 promotes lateral root emergence. *Nat. Cell Biol.* **10,** 946–954 CrossRef Medline
9. Geisler, M., Bailly, A., and Ivanchenko, M. (2016) Master and servant: Regulation of auxin transporters by FKBPs and cyclophilins. *Plant Sci.* **245,** 1–10 CrossRef Medline
10. Grones, P., and Friml, J. (2015) Auxin transporters and binding proteins at a glance. *J. Cell Sci.* **128,** 1–7 CrossRef Medline
11. Geisler, M., and Murphy, A. S. (2006) The ABC of auxin transport: The role of p-glycoproteins in plant development. *FEBS Lett.* **580,** 1094–1102 CrossRef Medline
12. Bouchard, R., Bailly, A., Blakeslee, J. J., Oehring, S. C., Vincenzetti, V., Lee, O. R., Paponov, I., Palme, K., Mancuso, S., Murphy, A. S., Schulz, B., and Geisler, M. (2006) Immunophilin-like TWISTED DWARF1 modulates auxin efflux activities of Arabidopsis P-glycoproteins. *J. Biol. Chem.* **281,** 30603–30612 CrossRef Medline
13. Santelia, D., Vincenzetti, V., Azzarello, E., Bovet, L., Fukao, Y., Düchtig, P., Mancuso, S., Martinoia, E., and Geisler, M. (2005) MDR-like ABC transporter AtPGP4 is involved in auxin-mediated lateral root and root hair development. *FEBS Lett.* **579,** 5399–5406 CrossRef Medline
14. Geisler, M., Blakeslee, J. J., Bouchard, R., Lee, O. R., Vincenzetti, V., Bandyopadhyay, A., Titapiwatanakun, B., Peer, W. A., Bailly, A., Richards, E. L., Ejendal, K. F., Smith, A. P., Baroux, C., Grossniklaus, U., Müller, A., *et al.* (2005) Cellular efflux of auxin catalyzed by the Arabidopsis MDR/PGP transporter AtPGP1. *Plant J.* **44,** 179–194 CrossRef Medline
15. Zhang, Y., Nasser, V., Pisanty, O., Omary, M., Wulff, N., Di Donato, M., Tal, I., Hauser, F., Hao, P., Roth, O., Fromm, H., Schroeder, J. I., Geisler, M., Nour-Eldin, H. H., and Shani, E. (2018) A transportome-scale amiRNA-based screen identifies redundant roles of Arabidopsis ABCB6 and ABCB20 in auxin transport. *Nat. Commun.* **9,** 4204 CrossRef Medline
16. Kamimoto, Y., Terasaka, K., Hamamoto, M., Takanashi, K., Fukuda, S., Shitan, N., Sugiyama, A., Suzuki, H., Shibata, D., Wang, B., Pollmann, S., Geisler, M., and Yazaki, K. (2012) Arabidopsis ABCB21 is a facultative auxin importer/exporter regulated by cytoplasmic auxin concentration. *Plant Cell Physiol.* **53,** 2090–2100 CrossRef Medline
17. Kaneda, M., Schuetz, M., Lin, B. S., Chanis, C., Hamberger, B., Western, T. L., Ehlting, J., and Samuels, A. L. (2011) ABC transporters coordinately expressed during lignification of Arabidopsis stems include a set of ABCBs associated with auxin transport. *J. Exp. Bot.* **62,** 2063–2077 CrossRef Medline
18. Santelia, D., Henrichs, S., Vincenzetti, V., Sauer, M., Bigler, L., Klein, M., Bailly, A., Lee, Y., Friml, J., Geisler, M., and Martinoia, E. (2008) Flavonoids redirect PIN-mediated polar auxin fluxes during root gravitropic responses. *J. Biol. Chem.* **283,** 31218–31226 CrossRef Medline
19. Terasaka, K., Blakeslee, J. J., Titapiwatanakun, B., Peer, W. A., Bandyopadhyay, A., Makam, S. N., Lee, O. R., Richards, E. L., Murphy, A. S., Sato, F.,

and Yazaki, K. (2005) PGP4, an ATP binding cassette P-glycoprotein, catalyzes auxin transport in Arabidopsis thaliana roots. *Plant Cell* **17,** 2922–2939 CrossRef Medline

20. Bainbridge, K., Guyomarc'h, S., Bayer, E., Swarup, R., Bennett, M., Mandel, T., and Kuhlemeier, C. (2008) Auxin influx carriers stabilize phyllotactic patterning. *Genes Dev.* **22,** 810–823 CrossRef Medline
21. Ofori, P. A., Geisler, M., di Donato, M., Pengchao, H., Otagaki, S., Matsumoto, S., and Shiratake, K. (2018) Tomato ATP-binding cassette transporter SlABCB4 is involved in auxin transport in the developing fruit. *Plants* **7,** 65 CrossRef Medline
22. Xu, Y., Zhang, S., Guo, H., Wang, S., Xu, L., Li, C., Qian, Q., Chen, F., Geisler, M., Qi, Y., and Jiang, D. A. (2014) OsABCB14 functions in auxin transport and iron homeostasis in rice (*Oryza sativa* L.). *Plant J.* **79,** 106–117 CrossRef Medline
23. Lee, M., Choi, Y., Burla, B., Kim, Y. Y., Jeon, B., Maeshima, M., Yoo, J. Y., Martinoia, E., and Lee, Y. (2008) The ABC transporter AtABCB14 is a malate importer and modulates stomatal response to CO2. *Nat. Cell Biol.* **10,** 1217–1223 CrossRef Medline
24. Titapiwatanakun, B., and Murphy, A. S. (2009) Post-transcriptional regulation of auxin transport proteins: Cellular trafficking, protein phosphorylation, protein maturation, ubiquitination, and membrane composition. *J. Exp. Bot.* **60,** 1093–1107 CrossRef Medline
25. Geisler, M., Wang, B., and Zhu, J. (2014) Auxin transport during root gravitropism: Transporters and techniques. *Plant Biol.* **16,** Suppl. 1, 50–57 CrossRef Medline
26. Henrichs, S., Wang, B., Fukao, Y., Zhu, J., Charrier, L., Bailly, A., Oehring, S. C., Linnert, M., Weiwad, M., Endler, A., Nanni, P., Pollmann, S., Mancuso, S., Schulz, A., and Geisler, M. (2012) Regulation of ABCB1/PGP1-catalysed auxin transport by linker phosphorylation. *EMBO J.* **31,** 2965–2980 CrossRef Medline
27. Christie, J. M., Yang, H., Richter, G. L., Sullivan, S., Thomson, C. E., Lin, J., Titapiwatanakun, B., Ennis, M., Kaiserli, E., Lee, O. R., Adamec, J., Peer, W. A., and Murphy, A. S. (2011) phot1 inhibition of ABCB19 primes lateral auxin fluxes in the shoot apex required for phototropism. *PLoS Biol.* **9,** e1001076 CrossRef Medline
28. Rademacher, E. H., and Offringa, R. (2012) Evolutionary adaptations of plant AGC kinases: From light signaling to cell polarity regulation. *Front. Plant Sci.* **3,** 250 CrossRef Medline
29. Ivanchenko, M. G., Zhu, J., Wang, B., Medvecká, E., Du, Y., Azzarello, E., Mancuso, S., Megraw, M., Filichkin, S., Dubrovsky, J. G., Friml, J., and Geisler, M. (2015) The cyclophilin A DIAGEOTROPICA gene affects auxin transport in both root and shoot to control lateral root formation. *Development* **142,** 712–721 CrossRef Medline
30. Xi, W., Gong, X., Yang, Q., Yu, H., and Liou, Y. C. (2016) Pin1At regulates PIN1 polar localization and root gravitropism. *Nat. Commun.* **7,** 10430 CrossRef Medline
31. Wang, B., Bailly, A., Zwiewka, M., Henrichs, S., Azzarello, E., Mancuso, S., Maeshima, M., Friml, J., Schulz, A., and Geisler, M. (2013) Arabidopsis TWISTED DWARF1 functionally interacts with auxin exporter ABCB1 on the root plasma membrane. *Plant Cell* **25,** 202–214 CrossRef Medline
32. Wu, G., Otegui, M. S., and Spalding, E. P. (2010) The ER-localized TWD1 immunophilin is necessary for localization of multidrug resistance-like proteins required for polar auxin transport in Arabidopsis roots. *Plant Cell* **22,** 3295–3304 CrossRef Medline
33. Geisler, M., and Bailly, A. (2007) Tête-à-tête: The function of FKBPs in plant development. *Trends Plant. Sci.* **12,** 465–473 CrossRef Medline
34. Bailly, A., Sovero, V., and Geisler, M. (2006) The Twisted Dwarf's ABC: How immunophilins regulate auxin transport. *Plant Signal. Behav.* **1,** 277–280 CrossRef Medline
35. Kamphausen, T., Fanghänel, J., Neumann, D., Schulz, B., and Rahfeld, J. U. (2002) Characterization of Arabidopsis thaliana AtFKBP42 that is membrane-bound and interacts with Hsp90. *Plant J.* **32,** 263–276 CrossRef Medline
36. Geisler, M., Kolukisaoglu, H. U., Bouchard, R., Billion, K., Berger, J., Saal, B., Frangne, N., Koncz-Kalman, Z., Koncz, C., Dudler, R., Blakeslee, J. J., Murphy, A. S., Martinoia, E., and Schulz, B. (2003) TWISTED DWARF1, a unique plasma membrane-anchored immunophilin-like protein, interacts with Arabidopsis multidrug resistance-like transporters AtPGP1 and AtPGP19. *Mol. Biol. Cell* **14,** 4238–4249 CrossRef Medline
37. Banasavadi-Siddegowda, Y. K., Mai, J., Fan, Y., Bhattacharya, S., Giovannucci, D. R., Sanchez, E. R., Fischer, G., and Wang, X. (2011) FKBP38 peptidylprolyl isomerase promotes the folding of cystic fibrosis transmembrane conductance regulator in the endoplasmic reticulum. *J. Biol. Chem.* **286,** 43071–43080 CrossRef Medline
38. Aryal, B., Laurent, C., and Geisler, M. (2015) Learning from each other: ABC transporter regulation by protein phosphorylation in plant and mammalian systems. *Biochem. Soc. Trans.* **43,** 966–974 CrossRef Medline
39. Pankow, S., Bamberger, C., Calzolari, D., Martínez-Bartolomé, S., Lavallée-Adam, M., Balch, W. E., and Yates, J. R., 3rd (2015) F508 CFTR interactome remodelling promotes rescue of cystic fibrosis. *Nature* **528,** 510–516 CrossRef Medline
40. Cant, N., Pollock, N., and Ford, R. C. (2014) CFTR structure and cystic fibrosis. *Int. J. Biochem. Cell Biol.* **52,** 15–25 CrossRef Medline
41. Pranke, I. M., and Sermet-Gaudelus, I. (2014) Biosynthesis of cystic fibrosis transmembrane conductance regulator. *Int. J. Biochem. Cell Biol.* **52,** 26–38 CrossRef Medline
42. Hutt, D. M., Roth, D. M., Chalfant, M. A., Youker, R. T., Matteson, J., Brodsky, J. L., and Balch, W. E. (2012) FK506 binding protein 8 peptidylprolyl isomerase activity manages a late stage of cystic fibrosis transmembrane conductance regulator (CFTR) folding and stability. *J. Biol. Chem.* **287,** 21914–21925 CrossRef Medline
43. Edlich, F., Erdmann, F., Jarczowski, F., Moutty, M. C., Weiwad, M., and Fischer, G. (2007) The Bcl-2 regulator FKBP38-calmodulin-Ca2+ is inhibited by Hsp90. *J. Biol. Chem.* **282,** 15341–15348 CrossRef Medline
44. Edlich, F., Weiwad, M., Erdmann, F., Fanghänel, J., Jarczowski, F., Rahfeld, J. U., and Fischer, G. (2005) Bcl-2 regulator FKBP38 is activated by Ca2+/calmodulin. *EMBO J.* **24,** 2688–2699 CrossRef Medline
45. Hemenway, C. S., and Heitman, J. (1996) Immunosuppressant target protein FKBP12 is required for P-glycoprotein function in yeast. *J. Biol. Chem.* **271,** 18527–18534 CrossRef Medline
46. Bailly, A., Sovero, V., Vincenzetti, V., Santelia, D., Bartnik, D., Koenig, B. W., Mancuso, S., Martinoia, E., and Geisler, M. (2008) Modulation of P-glycoproteins by auxin transport inhibitors is mediated by interaction with immunophilins. *J. Biol. Chem.* **283,** 21817–21826 CrossRef Medline
47. Bailly, A., Yang, H., Martinoia, E., Geisler, M., and Murphy, A. S. (2011) Plant lessons: Exploring ABCB functionality through structural modeling. *Front. Plant Sci.* **2,** 108 CrossRef Medline
48. Hrycyna, C. A., Airan, L. E., Germann, U. A., Ambudkar, S. V., Pastan, I., and Gottesman, M. M. (1998) Structural flexibility of the linker region of human P-glycoprotein permits ATP hydrolysis and drug transport. *Biochemistry* **37,** 13660–13673 CrossRef Medline
49. Hwang, J. U., Song, W. Y., Hong, D., Ko, D., Yamaoka, Y., Jang, S., Yim, S., Lee, E., Khare, D., Kim, K., Palmgren, M., Yoon, H. S., Martinoia, E., and Lee, Y. (2016) Plant ABC transporters enable many unique aspects of a terrestrial plant's lifestyle. *Mol. Plant* **9,** 338–355 CrossRef Medline
50. Multani, D. S., Briggs, S. P., Chamberlin, M. A., Blakeslee, J. J., Murphy, A. S., and Johal, G. S. (2003) Loss of an MDR transporter in compact stalks of maize br2 and sorghum dw3 mutants. *Science* **302,** 81–84 CrossRef Medline
51. Lu, X., Dittgen, J., Piślewska-Bednarek, M., Molina, A., Schneider, B., Svatoš, A., Doubský, J., Schneeberger, K., Weigel, D., Bednarek, P., and Schulze-Lefert, P. (2015) Mutant allele-specific uncoupling of PENETRATION3 functions reveals engagement of the ATP-binding cassette transporter in distinct tryptophan metabolic pathways. *Plant Physiol.* **168,** 814–827 CrossRef Medline
52. Holland, I. B., and Blight, M. A. (1999) ABC-ATPases, adaptable energy generators fuelling transmembrane movement of a variety of molecules organisms from bacteria to humans. *J. Mol. Biol.* **293,** 381–399 CrossRef Medline
53. Chang, G. (2003) Multidrug resistance ABC transporters. *FEBS Lett.* **555,** 102–105 CrossRef Medline
54. Bailly, A., Wang, B., Zwiewka, M., Pollmann, S., Schenck, D., Lüthen, H., Schulz, A., Friml, J., and Geisler, M. (2014) Expression of TWISTED DWARF1 lacking its in-plane membrane anchor leads to increased cell

elongation and hypermorphic growth. *Plant J.* **77,** 108–118 CrossRef Medline
55. Dacres, H., Wang, J., Dumancic, M. M., and Trowell, S. C. (2010) Experimental determination of the Förster distance for two commonly used bioluminescent resonance energy transfer pairs. *Anal. Chem.* **82,** 432–435 CrossRef Medline
56. Ernst, R., Kueppers, P., Stindt, J., Kuchler, K., and Schmitt, L. (2010) Multidrug efflux pumps: Substrate selection in ATP-binding cassette multidrug efflux pumps—first come, first served? *FEBS J.* **277,** 540–549 CrossRef Medline
57. Dawson, R. J., and Locher, K. P. (2007) Structure of the multidrug ABC transporter Sav1866 from *Staphylococcus aureus* in complex with AMP-PNP. *FEBS Lett.* **581,** 935–938 CrossRef Medline
58. Currier, S. J., Kane, S. E., Willingham, M. C., Cardarelli, C. O., Pastan, I., and Gottesman, M. M. (1992) Identification of residues in the first cytoplasmic loop of P-glycoprotein involved in the function of chimeric human MDR1-MDR2 transporters. *J. Biol. Chem.* **267,** 25153–25159 Medline
59. Kim, J. Y., Henrichs, S., Bailly, A., Vincenzetti, V., Sovero, V., Mancuso, S., Pollmann, S., Kim, D., Geisler, M., and Nam, H. G. (2010) Identification of an ABCB/P-glycoprotein-specific inhibitor of auxin transport by chemical genomics. *J. Biol. Chem.* **285,** 23309–23317 CrossRef Medline
60. Billet, A., Mornon, J. P., Jollivet, M., Lehn, P., Callebaut, I., and Becq, F. (2013) CFTR: Effect of ICL2 and ICL4 amino acids in close spatial proximity on the current properties of the channel. *J. Cyst. Fibros.* **12,** 737–745 CrossRef Medline
61. MacArthur, M. W., and Thornton, J. M. (1991) Influence of proline residues on protein conformation. *J. Mol. Biol.* **218,** 397–412 CrossRef Medline
62. Sheppard, D. N., Travis, S. M., Ishihara, H., and Welsh, M. J. (1996) Contribution of proline residues in the membrane-spanning domains of cystic fibrosis transmembrane conductance regulator to chloride channel function. *J. Biol. Chem.* **271,** 14995–15001 CrossRef Medline
63. Geisler, M., Girin, M., Brandt, S., Vincenzetti, V., Plaza, S., Paris, N., Kobae, Y., Maeshima, M., Billion, K., Kolukisaoglu, U. H., Schulz, B., and Martinoia, E. (2004) Arabidopsis immunophilin-like TWD1 functionally interacts with vacuolar ABC transporters. *Mol. Biol. Cell* **15,** 3393–3405 CrossRef Medline
64. Ni, Z., Bikadi, Z., Shuster, D. L., Zhao, C., Rosenberg, M. F., and Mao, Q. (2011) Identification of proline residues in or near the transmembrane helices of the human breast cancer resistance protein (BCRP/ABCG2) that are important for transport activity and substrate specificity. *Biochemistry* **50,** 8057–8066 CrossRef Medline
65. Mravec, J., Kubes, M., Bielach, A., Gaykova, V., Petrásek, J., Skůpa, P., Chand, S., Benková, E., Zazímalová, E., and Friml, J. (2008) Interaction of PIN and PGP transport mechanisms in auxin distribution-dependent development. *Development* **135,** 3345–3354 CrossRef Medline
66. Zhu, J., Bailly, A., Zwiewka, M., Sovero, V., Di Donato, M., Ge, P., Oehri, J., Aryal, B., Hao, P., Linnert, M., Burgardt, N. I., Lücke, C., Weiwad, M., Michel, M., Weiergräber, O. H., *et al.* (2016) TWISTED DWARF1 mediates the action of auxin transport inhibitors on actin cytoskeleton dynamics. *Plant Cell* **28,** 930–948 CrossRef Medline
67. Baginski, E. S., Epstein, E., and Zak, B. (1975) Review of phosphate methodologies. *Ann. Clin. Lab. Sci.* **5,** 399–416 Medline